DALTON
FULL PAPER

Ruthenium-(II)/-(III) terpyridine complexes incorporating imine functionalities. Synthesis, structure, spectroscopic and electrochemical properties †

Biplab Mondal, Soma Chakraborty, Pradip Munshi, Mrinalini G. Walawalkar and Goutam Kumar Lahiri *

Department of Chemistry, Indian Institute of Technology, Bombay, Mumbai-400076, India

Received 12th January 2000, Accepted 15th May 2000
Published on the Web 22nd June 2000

A new class of ruthenium terpyridine complexes of the type $[Ru^{II}(trpy)(L^{1-6})Cl]$ **1**–**6** (trpy = 2, 2′ : 6′, 2″-terpyridine; L^{1-3} = *o*-$^{-}OC_6H_3(R)C(R')=NCH_2C_6H_5$ and L^{4-6} = *o*-$^{-}OC_6H_3(R)CH(R')N=NC_6H_5$; where R = H or *p*-$NO_2$ and R′ = H or CH_3) have been synthesized. The "free" ligands incorporating a NH spacer *o*-$^{-}OC_6H_3(R)C(R')=NNHC_6H_5$ (HL^{4-6}) have undergone imine to azo tautomerism on co-ordination to the ruthenium terpyridine moiety in the complexes **4**–**6**, whereas those having a CH_2 spacer (HL^{1-3}) remain unaltered on co-ordination. The diamagnetic, neutral complexes **1**–**6** exhibit strong MLCT transitions in the visible region and intraligand transitions in the UV region. A significant shift in MLCT band energy has been observed depending on the ligand field strength of the co-ordinated L. The complexes display a reversible ruthenium(III)–ruthenium(II) couple in the potential range of 0.12–0.63 V and a quasi-reversible ruthenium(IV)–ruthenium(III) couple in the range of 1.21–1.85 V *versus* SCE. The higher ligand field strength of the co-ordinated L^{4-6} compared to the co-ordinated L^{1-3} is reflected in the observed metal redox processes. The reduction of the co-ordinated terpyridine has been observed near −1.3 V. The complexes exhibit moderately strong emissions from the lowest energy MLCT bands in the range 661–690 nm in EtOH–MeOH (4 : 1 v/v) at 77 K. The quantum yields of the complexes (Φ = 0.006–0.09) are found to be reasonably sensitive to the nature of the co-ordinated L. The oxidised complexes $\mathbf{3}^{+}$ and $\mathbf{6}^{+}$ have been isolated in the solid state as their perchlorate salts. The crystal structure of $\mathbf{3}^{+}$ exhibits pseudo-octahedral *trans* geometry with regard to the relative disposition of the imine nitrogen (N4) of L^3 and the central pyridyl group of the trpy ligand. The one-electron paramagnetic complexes show 1 : 1 conductivity and display ligand-to-metal charge transfer bands near 600 and 400 nm and intraligand transitions in the UV region. The observed rhombic EPR spectra at 77 K corresponding to the distorted octahedral geometry have been analysed to furnish values of axial (Δ) and rhombic (V) distortion parameters as well as the energies of the two expected ligand field transitions (v_1 and v_2) within the t_2 shell.

Introduction

The development of new photo-redox active ruthenium polypyridine derivatives has been the subject of continuous research activity.[1] Facile electron-transfer properties, strong metal to ligand charge-transfer absorptions and long lived ^{3}MLCT excited states of this class of complexes make them attractive for the development of photochemical and electrochemical devices.[2] In this regard a variety of ruthenium bipyridine and phenanthroline complexes have been synthesized and studied extensively over the last three decades in order to modulate their photochemical and photophysical properties.[3] However, the corresponding terpyridine complexes have not been explored to that extent.[4] Although the terpyridine type of tridentate ligand has structural advantages over bidentate bipyridine and phenanthroline ligands, it has a serious drawback from the photophysical point of view.[5] As compared to bipyridine ligands the bite angles of terpyridine ligands are not ideally suited for octahedral co-ordination and this in turn results in a relatively weak ligand field and low energy metal centred states.[6] In consequence ruthenium terpyridine complexes exhibit relatively short lived MLCT states and behave as weak emitters compared to the analogous bipyridine complexes (τ = 890 ns, 250 ps and $\Phi = 0.054$, $\leq 5 \times 10^{-6}$ for $Ru(bpy)_3^{2+}$ and $Ru(trpy)_2^{2+}$ respectively at room temperature).[7] Since the short lifetime of ruthenium terpyridine complexes is known to originate essentially from the small energy gap between the emitting ^{3}MLCT state and the upper lying ^{3}MC state, an increase in energy gap would therefore be desirable. This can be achieved by introducing either suitable substituents in the terpyridine framework itself or by using ancillary ligands, L along with the ruthenium monoterpyridine core.[8]

The present work originates from our interest in introducing phenolic Schiff base ligands HL having CH_2 and NH spacers $[HOC_6H_3(R)C(R')=NCH_2C_6H_5$ (**A**) and $HOC_6H_3(R)C(R') = NNHC_6H_5$ (**B**)] as ancillary ligands to develop mixed ligand ruthenium–terpyridine complexes of the type [Ru(trpy)(L)(Cl)]. Although both types of ligands (**A** and **B**) are known to be stable enough either in the free state or on co-ordination, here the ligands having the NH spacer (**B**) undergo internal imine to azo tautomerism on chelation to the ruthenium–terpyridine moiety. To the best of our knowledge this work demonstrates the first example of ruthenium–terpyridine complexes incorporating imine functionalities. Herein we report the synthetic aspects of complexes of type $[Ru^{II/III}(trpy)(L)(Cl)]$, their spectroscopic and electron-transfer properties, the crystal structure of one trivalent complex $[Ru^{III}(trpy)(L^3)(Cl)]ClO_4$, the spectro-electrochemical correlation and solution electronic structure of the trivalent complexes.

Results and discussion

Synthesis and spectral properties

The six phenolic Schiff base ligands used are classified into two groups, HL^1–HL^3 (**A**) and HL^4–HL^6 (**B**), depending on the

† Electronic supplementary information (ESI) available: IR spectra; analytical, spectral, electrochemical and emission data. See http://www.rsc.org/suppdata/dt/b0/b000257g/

DOI: 10.1039/b000257g

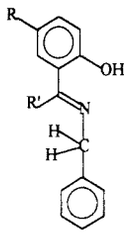

A

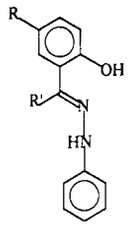

B

R= H, R′ = H → HL^1 R= H, R′ = H → HL^4

R= H, R′ = CH_3 → HL^2 R= H, R′ = CH_3 → HL^5

R= NO_2, R′ = H → HL^3 R= NO_2, R′ = H → HL^6

nature of the spacer (CH_2 or NH) present in between the imine nitrogen and the phenyl ring and within each group the three ligands differ with respect to the substituents either on the phenolic ring or on the imine fragment. The complexes [Ru^{II}(trpy)(L)(Cl)] **1**–**6** (trpy = 2,2′ : 6′,2″-terpyridine) have been synthesized from [Ru(trpy)Cl_3] following the general dechlorination synthetic route as shown in Scheme 1. The dark coloured

$Ru^{III}(trpy)Cl_3 + HL \xrightarrow{(i)} [Ru^{II}(trpy)(L)(Cl)]$

Ligand	Complex
L^1	**1**
L^2	**2**
L^3	**3**
L^4	**4**
L^5	**5**
L^6	**6**

Scheme 1 (i) MeOH, CH_3CO_2Na, heat.

pure neutral complexes [Ru(trpy)(L^3)(Cl)] **3** and [Ru(trpy)-(L^6)(Cl)] **6** are precipitated directly from the reaction mixture, whereas the other four complexes (**1, 2, 4** and **5**) are obtained on removal of solvent followed by chromatographic purification using a silica gel column. The microanalytical data of the complexes confirm the gross composition of the mixed chelates [Ru^{II}(trpy)(L)(Cl)] **1**–**6**. The diamagnetic complexes are non-conducting in acetonitrile solution. The FAB mass spectra of two representative complexes, **3** and **6** (one from each class), have been recorded. The maximum molecular peaks are observed at *m*/*z* 625 and 626.7 for **3** and **6** respectively, which match well with the corresponding calculated masses (625.8 and 626.9).

The anionic form of the ancillary ligands of type **A** is observed to be retained in complexes **1**–**3** whereas the ligands of type **B** (L^4–L^6) have undergone imine ⟶ azo tautomerism during the reaction (Scheme 1) which eventually leads to the formation of complexes of type **C** (see NMR part). It may be

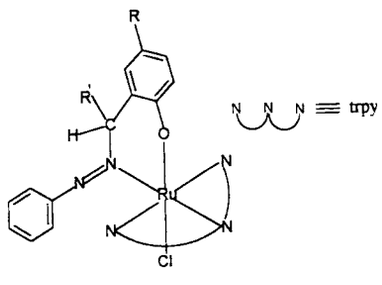

C

noted that the anionic form of ligands (L^{4-6}) is found to be stable in other ruthenium complexes and also remains unchanged in the presence of sodium acetate, but in absence of [Ru(trpy)Cl_3], under hot methanolic reaction conditions (Scheme 1). This implies that the tautomerism of L^- takes place particularly on co-ordination to the Ru(trpy)Cl_3 moiety. The observed imine (**D**) ⟶ azo (**E**) tautomerism of the co-ordinated L^- in complexes **4**–**6** may be compared with the allylic rearrangement (**F**–**G**) of alkene derivatives.[9] The inert-

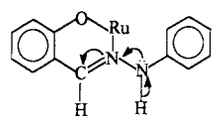

D

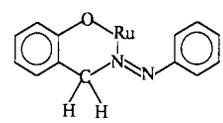

E

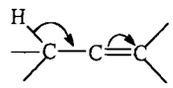

F

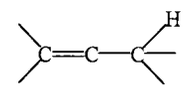

G

ness of the "free" ligands H_2L^{4-6} with respect to tautomerism compared with their behaviour in the complexes **4**–**6** is presumably due to the basic nature of the NH nitrogen atom. On chelation the nitrogen centre becomes less basic which in turn facilitates migration of the acidic NH proton from the nitrogen atom to the carbon concerned.

The unsymmetrical nature of L^- leads to the possibility of two isomeric forms, **H** and **I**, of the complexes [Ru(trpy)(L)-

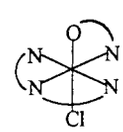

H

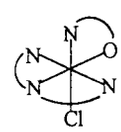

I

(Cl)].[10] In practice both isomers have been noticed in solution as an intimate mixture for the complexes **1**, **2**, **4** and **5** (see NMR part). All our attempts to separate them by column chromatography have failed. Therefore, data are reported here only for the isomerically pure complexes, **3** and **6**.

The three notable features of the infrared spectra are: (i) The "free" ligands HL^4–HL^6 display one sharp band near 3300 cm^{-1} corresponding to the $\nu_{N\text{-}H}$ frequency[11] which is systematically absent for the corresponding complexes (**4**–**6**); (ii) the formation of the N=N bond in the ligand framework present in complexes **4**–**6** is evidenced by the appearance of a new strong and sharp band near 1300 cm^{-1};[12] thus the formation of a new N=N bond at the expense of the $\nu_{N\text{-}H}$ frequency supports the structure **C** of **4**–**6**; (iii) complexes **1**–**6** exhibit one sharp band near 335 cm^{-1} due to the Ru^{II}–Cl stretching frequency, as expected.[13]

The ^{1}H NMR spectra of two representative complexes **1** and **4** are shown in Fig. 1. The absence of the O–H proton of the "free" ligands HL^1–HL^6 in the spectra of the complexes suggests co-ordination through the phenolato oxygen of L^-. The methylene protons (CH_2) of L^{1-3} in complexes **1**–**3** appear near δ 5.95 as a singlet (Fig. 1a) which is reasonably deshielded as compared to that of the "free" ligands (δ 4.85).[14] The methyl signal of **2** appears at δ 2.39 as a singlet. The N–H proton of the "free" ligands HL^4–HL^6 appears near δ 7.7 as a broad singlet,[11] however, this signal is absent in the spectra of complexes **4**–**6**.[14] On the other hand a new singlet corresponding to two protons for **4** and **6** and a multiplet corresponding to one proton for **5** appeared near δ 3.8, which are assigned to the H_2CN=N and $HC(CH_3)$N=N protons respectively. The methyl protons of complex **5** are observed at δ 2.35 as a doublet.

The presence of asymmetric ligands L^- in the complexes make all the five aromatic rings inequivalent. The complexes **1**, **2**, **4**, **5**, and **3**, **6** thus possessing twenty and nineteen non-equivalent aromatic protons respectively. Since the electronic

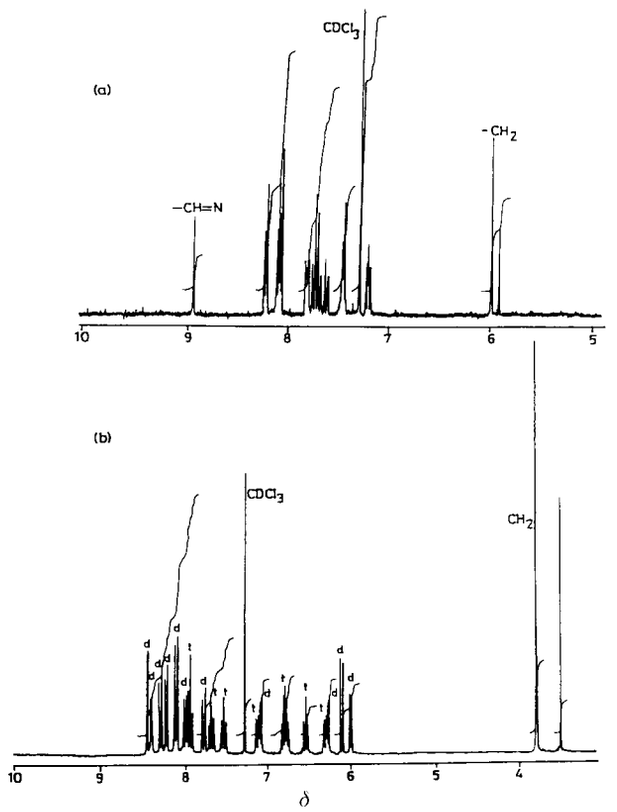

Fig. 1 ^{1}H NMR spectra of (a) [Ru^{II}(trpy)(L^1)Cl] **1** and (b) [Ru^{II}(trpy)(L^4)Cl] **4** in $CDCl_3$.

environments of many aromatic hydrogen atoms are similar, their signals may appear in a narrow chemical shift range. In fact the aromatic regions of the spectra of complexes **1**–**3** are complicated due to overlapping of several signals (Fig. 1a) which has precluded the identification of the individual protons. However, for **4**–**6** the peaks are reasonably separated and all the doublets, triplets and singlet have clearly been assigned (Fig. 1b). The direct comparison of the intensity of the aromatic proton signals with that of the clearly observable aliphatic (CH_2) protons reveals the presence of the calculated number of aromatic protons in the complexes.

The azomethine (CH=N) proton of complexes **1** and **3** has clearly been observed near δ 9.0 as a singlet (Fig. 1a) which is considerably deshielded relative to that of the "free" ligands ($\delta \approx 8.4$) as a consequence of electron donation to the metal centre.[15] The azomethine proton (CH=N) of the "free ligands" HL^4 and HL^6 is found to be absent in the NMR spectra of the corresponding complexes **4** and **6** (Fig. 1b). Therefore this absence as well as the absence of the N–H proton in all the three complexes **4**–**6** and the simultaneous appearance of the new C–H proton signal in the upfield region (δ 3.8) strongly support the internal imine ⟶ azo tautomerism (**D** ⟶ **E**) of the ligands L^4–L^6 in these complexes.

The presence of an intimate mixture of the two isomers **H** and **I** for complexes **1**, **2**, **4** and **5** in a ratio of $\approx 2:1$ in solution has been revealed from the well resolved two distinct upfield methylene (CH_2) proton signals and the direct comparison of the intensity of the methylene protons with that of the aromatic protons (Fig. 1).

In dichloromethane solution the complexes exhibit two moderately intense transitions in the visible region and three intense transitions in the uv region (Table 1). The lowest energy transition is associated with a shoulder to even further lower energy (Table 1, Fig. 2). The visible region transitions are assigned to dπ(Ru^{II}) ⟶ π^*(trpy) MLCT transitions,[16] their energy varying depending on the nature of the ancillary ligands (L). In addition each complex exhibits an assortment of three intense

Table 1 Electronic spectral data in dichloromethane

Complex	UV/VIS λ_{max}/nm (ε/dm^3 mol^{-1} cm^{-1})
3	583 (10800), 429 (13090), 324 (34370), 282 (24660), 240 (47250)
6	530 (5320), 404 (4250), 316 (15960), 275 (19680), 234 (22130)
3$^+$	1600 (90), 600 (5170), 420 (8890), 310 (25850), 275 (22960), 230 (41360)
6$^+$	1080 (70), 570 (4300), 400 (7820), 307 (20220), 272 (23580), 217 (32320)

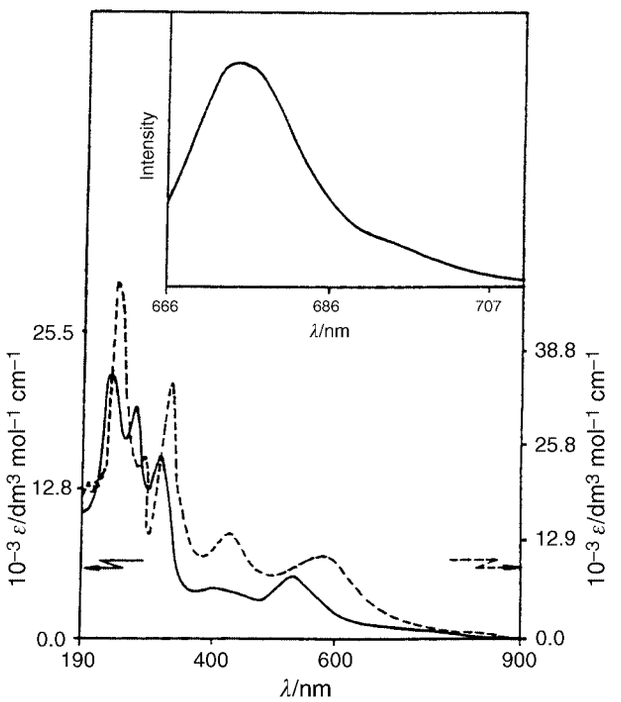

Fig. 2 Electronic spectra of [Ru^{II}(trpy)(L^3)Cl] **3** (------) and [Ru^{II}(trpy)(L^6)Cl] **6** (——) in dichloromethane. The inset shows the emission spectrum of **3** in EtOH–MeOH, 4 : 1 (v/v) at 77 K.

transitions in the higher energy region which are believed to be the ligand centred $\pi \longrightarrow \pi^*$ transitions.[16]

The lowest energy MLCT band of $[Ru(trpy)_2]^{2+}$ appears at 478 nm.[17] Thus the replacement of one strong π-acidic terpyridine ligand by L$^-$ decreases the energy of the same transition, which is in consonance with the greater σ-donor and weaker π-acceptor property of L$^-$ relative to terpyridine. This red shift compared to $[Ru(trpy)_2]^{2+}$ is observed to be more prominent in **3** (having a CH_2 spacer) than in complex **6** and implies ligand L^6 exerts a greater ligand field strength compared to L^3. The presence of the azo group in the framework of co-ordinated L^6 might be responsible for the observed difference in field strength.[18] The observed difference in ligand field strength between the two types of ligands (L^3 and L^6) is also reflected in the metal redox processes (see later).

Electron-transfer properties

The complexes are electroactive with respect to metal as well as ligand centres and display the same three responses in the potential range of ±2.0 V *versus* SCE. The reduction potential data are listed in Table 2 and the representative voltammograms are shown in Fig. 3.

Ruthenium(III)-ruthenium(II) couple. In dichloromethane solution complex **3** displays a reversible ruthenium(III)–ruthenium(II) couple at 0.34 V whereas for **6** the same couple appears at 0.63 V.[14] The one-electron nature of the responses is established by constant potential coulometry (Table 2). The

Table 2 Electrochemical data at 298 K [a]

Complex	E°_{298}/V(ΔE_p/mV)			n [b]	ΔE° [c]/V	ν_{MLCT}/cm^{-1}	
	Ru^{III}–Ru^{II}	Ru^{IV}–Ru^{III}	ligand reduction			observed [d]	calculated [e]
3	0.34 (70)	1.71 (120)	−1.32 (80)	1.04	1.66	17152	16388
6	0.63 (70)	1.85 [f]	−1.38 (100)	1.03	2.01	18867	19210

[a] Solvent, dichloromethane; supporting electrolyte, $[NEt_4][ClO_4]$; reference electrode, SCE; solute concentration, 10^{-3} mol dm^{-3}; working electrode, platinum wire. Cyclic voltammetric data; scan rate, 50 mV s^{-1}; $E^\circ_{298} = 0.5\ (E_{pa} + E_{pc})$ where E_{pa} and E_{pc} are the anodic and cathodic peak potentials, respectively. [b] $n = Q/Q'$, where Q' is the calculated coulomb count for 1e$^-$ transfer and Q is the coulomb count found after exhaustive electrolysis of a $\approx 10^{-2}$ M solution of the complex. [c] Calculated by using eqn. (2) of text. [d] In dichloromethane solution. [e] Calculated by using eqn. (1) of text. [f] E_{pa} value is considered due to the irreversible nature of the voltammogram.

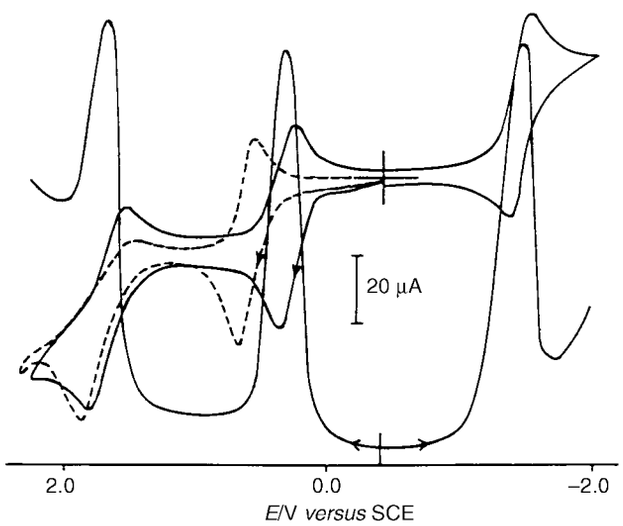

Fig. 3 Cyclic voltammograms of $\approx 10^{-3}$ mol dm^{-3} solutions of the complexes $[Ru^{II}(trpy)(L^2)Cl]$ **3** (——) and $[Ru^{II}(trpy)(L^6)Cl]$ **6** (------) in dichloromethane at 298 K. The reduction of co-ordinated terpyridine and differential pulse voltammograms are shown only for **3**.

presence of trivalent ruthenium in the oxidised solution is confirmed by the characteristic rhombic EPR spectra of the ruthenium(III) congeners (see later).[19] Although here the stability of the ruthenium(II) state is found to be greater in **6** as compared to **3**, the unaltered ligand L^6 (having NH spacer) results in a lower ruthenium(III)–ruthenium(II) potential compared to that with L^3 in $[Ru(bpy)_2L]$ complexes.[14] The observed reverse order of stability of the ruthenium(II) state in the present set of complexes might be due to the presence of the N=N group in the modified ligand framework of L^6 in **6,** as the π-acidic nature of the azo function helps to stabilise the lower oxidation state of the metal ion preferentially.[20] A potential shift of >300 mV has been observed while moving from **3** to **6**.

The ruthenium(III)–ruthenium(II) potential of $[Ru(trpy)_2]^{2+}$ appears at 1.30 V.[21] Therefore a decrease in 0.7–1.0 V of this couple depending on the nature of L has been observed while moving from $[Ru^{II}(trpy)_2]^{2+}$ to $[Ru^{II}(trpy)(L)(Cl)]$. The σ-donor nature of the phenolato group of L^- provides electrostatic stabilisation of the Ru^{III}–L species which has originated from the reduction of the overall charge of +2 in $[Ru(trpy)_2]^{2+}$ to 0 in the present complexes, $[Ru(trpy)(L)(Cl)]$.[22] The decrease in potential of the Ru^{III}–Ru^{II} couple and its reversible nature (Fig. 3) facilitates the isolation of the trivalent congeners, $[Ru^{III}(trpy)(L)(Cl)]^+$ with the present ligand set up.

Ruthenium(IV)–ruthenium(III) couple. The complexes display a second quasi reversible oxidation process near 2 V (Fig. 3). The observed potentials vary depending on the type of ligands (**A** and **B**) (Table 2). The one-electron nature of the process has been established with the help of differential pulse voltammetry, which shows the second oxidation process to have the same height as that of the first couple (Fig. 3). The oxidised species $[Ru(trpy)(L)(Cl)]^{2+}$ is found to be unstable on the coulometric timescale. The second oxidation process can tentatively be assigned to the $Ru^{III} \longrightarrow Ru^{IV}$ oxidation as the "free" ligands (HL) or their sodium salts (NaL) do not show any redox activity within the experimental potential range (± 2 V). Here the potential difference between the two successive oxidation processes is observed to be in the range 1.2–1.4 V which matches well with the average potential difference (1.1–1.5 V) between the two successive redox processes of ruthenium ($Ru^{II/III}$–$Ru^{III/IV}$) observed in other mononuclear ruthenium complexes.[23] However, the possibility of the oxidation of co-ordinated ligands cannot be ruled out.

Ligand reduction. The complexes exhibit one reversible reduction near −1.3 V (Table 2, Fig. 3). The one-electron stoichiometry of this process has been verified by differential pulse voltammetry. Since the "free" ligands (HL or NaL) do not show any reduction and the reduction of co-ordinated terpyridine is well documented,[24] the observed reduction is assigned to be that of co-ordinated terpyridine.

All our attempts to make suitable single crystals for X-ray characterisation of the complexes have failed. However, elemental analysis and FAB-mass data are consistent with the gross composition and IR and NMR data provide strong support in favour of the internal transformation of the ligand L^6 in complex **6**.

Trivalent ruthenium(III) congeners $[Ru^{III}(trpy)(L)(Cl)]^+$ 3^+ and 6^+

Coulometric oxidations of the complexes at a potential 150 mV positive of the corresponding E_{pa} of Ru^{III}–Ru^{II} couple in dichloromethane solution at 298 K result in green oxidised species $\mathbf{3}^+$ and $\mathbf{6}^+$. The observed Coulomb count corresponds to 1e$^-$ transfer for both complexes (Table 2). The oxidised complexes display voltammograms which are superposable on those of the corresponding bivalent complexes (**3** and **6**), implying that the oxidation here may be stereoretentive in nature. The trivalent complexes can quantitatively be reduced to the parent bivalent complexes **3** and **6**.

Chemical oxidations of complexes **3** and **6** by aqueous ammonium cerium(IV) sulfate and ammonium cerium(IV) sulfate in 0.1 M aqueous $HClO_4$ respectively result in the same green oxidised complexes ($\mathbf{3}^+$ and $\mathbf{6}^+$). That incorporating the ligand of type **A**, $\mathbf{3}^+$, is stable both in the solid and solution states whereas the complex having the ligand of type **B**, $\mathbf{6}^+$, is found to be reactive in the solution state. The observed stability order of $\mathbf{3}^+$ and $\mathbf{6}^+$ in the solution state is in accord with the $Ru^{II} \longrightarrow Ru^{III}$ oxidation potentials of the complexes (Table 2). The complexes $\mathbf{3}^+$ and $\mathbf{6}^+$ can be quantitatively reduced back to the parents **3** and **6** by hydrazine hydrate.

The complexes $\mathbf{3}^+$ and $\mathbf{6}^+$ have been isolated in the solid state as their monohydrated perchlorate salts, $[Ru^{III}(trpy)(L)(Cl)]$-$ClO_4 \cdot H_2O$. Their microanalytical data match well with the calculated values. The complexes exhibit 1 : 1 conductivity in

Table 3 Selected bond distances (Å) and angles (°) and their standard deviations for $[Ru(trpy)(L^3)Cl]ClO_4 \cdot 0{\cdot}5C_6H_6$ $\mathbf{3}^+$

Ru–N(1)	2.070(4)	Ru–O(1)	1.982(3)
Ru–N(2)	1.974(4)	Ru–Cl(1)	2.334(16)
Ru–N(3)	2.092(4)	C(22)–N(4)	1.289(6)
Ru–N(4)	2.100(4)	C(10)–O(1)	1.314(5)
N(2)–Ru–O(1)	88.21(4)	N(3)–Ru–N(4)	96.53(14)
N(2)–Ru–N(1)	79.20(15)	N(2)–Ru–Cl(1)	87.55(11)
O(1)–Ru–N(1)	87.18(14)	O(1)–Ru–Cl(1)	175.19(10)
N(2)–Ru–N(3)	79.56(15)	N(1)–Ru–Cl(1)	89.81(11)
O(1)–Ru–N(3)	91.34(14)	N(3)–Ru–Cl(1)	90.11(11)
N(1)–Ru–N(3)	158.75(15)	N(4)–Ru–Cl(1)	93.50(11)
N(2)–Ru–N(4)	175.96(14)	N(4)–C(22)–C(21)	127.6(4)
O(1)–Ru–N(4)	90.88(14)	C(10)–O(1)–Ru	127.6(3)
N(1)–Ru–N(4)	104.69(14)	C(22)–N(4)–Ru	122.1(3)

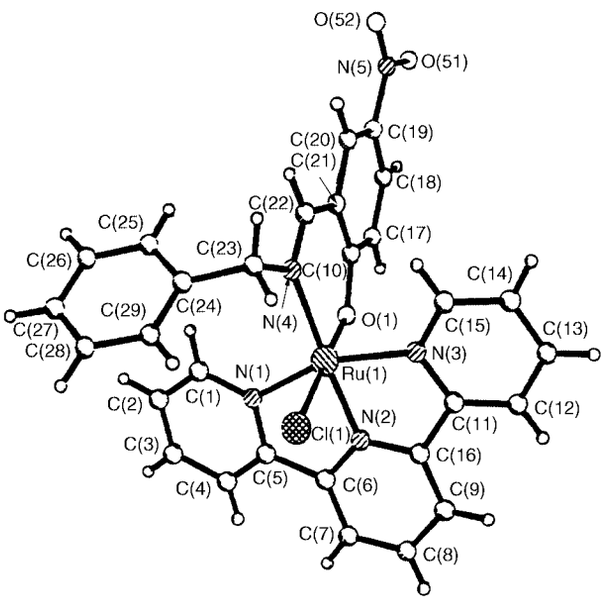

Fig. 4 An ORTEP[25] plot for $[Ru^{III}(trpy)(L^3)Cl]ClO_4$ $\mathbf{3}^+$. The benzene and perchlorate anion are removed for clarity.

acetonitrile at 298 K [Λ_M/Ω^{-1} cm^2 mol^{-1} 155 for $\mathbf{3}^+$ and 148 for $\mathbf{6}^+$]. The presence of perchlorate ion is evidenced by a strong and broad band near 1100 cm^{-1} and a sharp band near 630 cm^{-1} in the IR spectra of the complexes. The $\nu_{Ru^{III}\text{-}Cl}$ stretching frequency is observed near 340 cm^{-1} as a sharp singlet.

The molecular structure of complex $\mathbf{3}^+$ has been established by single-crystal X-ray diffraction. The crystal structure is shown in Fig. 4 and selected bond lengths and angles are listed in Table 3. The complex is monomeric and the lattice consists of one type of molecule. The crystal consists of an array of $[Ru(trpy)(L^3)Cl]^+$cations, $[ClO_4]^-$ anions and benzene of crystallisation in a 1:1:0.5 stoichiometry. The RuN_4OCl coordination sphere is distorted octahedral as can be seen from the angles subtended at the ruthenium centre and composed of a meridionally bound trpy ligand, a bidentate L^3 ligand and a chloride. The central pyridine of the trpy ligand is bound *trans* to the imine nitrogen (N4) (structure **I**) with an observed N(4)–Ru–N(2) angle of 175.96(14)°. The other two terminal pyridine rings of trpy bind to the ruthenium ion at angles N(1)–Ru–N(2) of 79.20(15) and N(3)–Ru–N(2) of 79.56(15)°, which indicates that due to structural constraint it cannot bind to ruthenium with an ideal (90°) geometry. The Ru–N(2) (central pyridine nitrogen of trpy) distance [1.974(4) Å] is shorter than the terminal Ru–N pyridine distances [Ru–N(1), 2.070(4) and Ru–N(3) 2.092(4) Å] as observed in other ruthenium–terpyridine complexes.[4] The Ru^{III}–N(trpy) bond distances found in this complex are similar to those reported for another known Ru^{III}-trpy complex $[trpy)(C_2O_4)Ru^{III}ORu^{III}(C_2O_4)(trpy)]\cdot 1.8H_2O$.[26] To the best of our knowledge this work represents

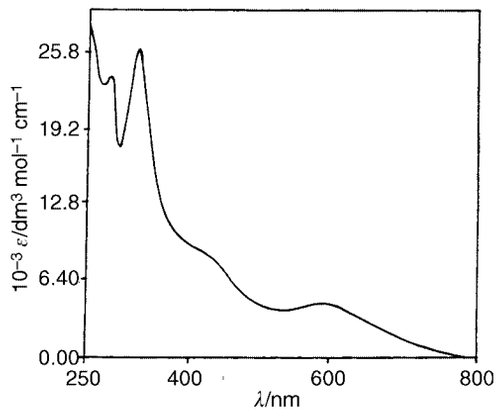

Fig. 5 Electronic spectrum of the oxidised complex $[Ru^{III}(trpy)(L^3)Cl][ClO_4]\cdot H_2O$ $\mathbf{3}^+$ in acetonitrile.

the first example of structurally characterised mononuclear ruthenium(III)–terpyridine complex as well as a ruthenium(III)–imine function. The Ru^{III}–O bond distance of 1.982(3) Å in $\mathbf{3}^+$ is significantly shorter than the Ru^{III}–O (phenolato) distance [2.112(5) Å] observed in the ruthenium(III)–orthometallated azophenol system (C–Ru–O in *trans* configuration)[27] but close to the average Ru^{III}–O(phenolato) distance, 1.981(2) Å, found in the ruthenium(III) salicylaldehydato complex.[23] The *trans* effect of the bound carbon atom was assigned to be the reason for the unusually long Ru^{III}–O distance in the azophenol complex. Thus this work demonstrates a good measure of a normal Ru^{III}–O(phenolato) distance. The Ru^{III}–Cl bond distance of 2.334(16) Å in $\mathbf{3}^+$ is similar to that reported for other Ru^{III}–Cl complexes.[28,29] The Ru^{III}–N(4) (imine nitrogen) distance in $\mathbf{3}^+$, 2.100(4) Å, merits scrutiny. No information on Ru^{III}–N(imine) bond lengths is available in the literature, but a case of Ru^{II}–N(imine) has been examined recently.[30] The latter distance is 2.039(4) Å which is significantly shorter than the Ru^{III}–N(4) distance in $\mathbf{3}^+$. The relatively short Ru–N(2)(trpy) distance *trans* to Ru–N(4)(imine) may account for the observed relatively long Ru^{III}–N(4)(imine) distance. The bond distance of C(22)–N(4) is 1.289(6) Å, which is normal for a C=N double bond.[31] The ClO_4^- anion is tetrahedral with an average Cl–O distance of 1.371(6) Å and an average O–Cl–O angle of 109.35°.

The complexes exhibit moderately strong ligand to metal charge-transfer (LMCT) transitions near 600 and 400 nm and in the uv region ligand based transitions (Table 1, Fig. 5).[28] The magnetic moment values of the complexes correspond to the low-spin d^5 configuration (μ_{eff}/μ_B; 1.93 for $\mathbf{3}^+$ and 1.88 for $\mathbf{6}^+$) and consequently the complexes display rhombic EPR spectra in dichloromethane–toluene glass (77 K) with distinct three g values (Fig. 6, Table 4).

The EPR spectra of the complexes have been analysed in terms of crystal field g-tensor theory of low-spin d^5 ions.[28,32] Among the parameters that can be derived from the theory are the splitting due to axial distortion (Δ) which transforms the t_2 shell into e + b (tetragonal distortion), the splitting due to rhombic distortion (V) which splits e further into non-degenerate components and the energies (ν_1 and ν_2) of the two optical transitions among the three Kramers doublets originating from the application of Δ, V and λ (spin–orbit coupling constant) on t_2 and the orbital reduction factor (k). The goodness of the analysis can be assessed by independent observation of the transitions ν_1 and ν_2 in optical spectra. The EPR spectra provide only the absolute g values and so neither their signs nor the correspondence of g_1, g_2 and g_3 to g_x, g_y and g_z are known. There are forty eight possible combinations based on the leveling (x, y, z) and the signs chosen for the experimentally observed g values. For the present case we have chosen the combination $-g_1 > -g_2 > g_3$ as this particular set gives the acceptable value of k (< 1.0). The value of k for all other combinations of g parameters does not fall within the limit of

Table 4 The EPR g values[a] and distortion parameters[b]

Complex	g_1	g_2	g_3	k	Δ/λ	V/λ	v_1/λ	v_2/λ	v_2/λ_{obs}
$\mathbf{3}^+$	−2.658	−2.067	1.691	0.778	4.258	−4.217	2.392	6.621	6.250
$\mathbf{6}^+$	−2.350	−2.054	1.887	0.639	6.987	−6.887	3.686	10.586	9.259

[a] In dichloromethane at 77 K. [b] Meanings are given in the text.

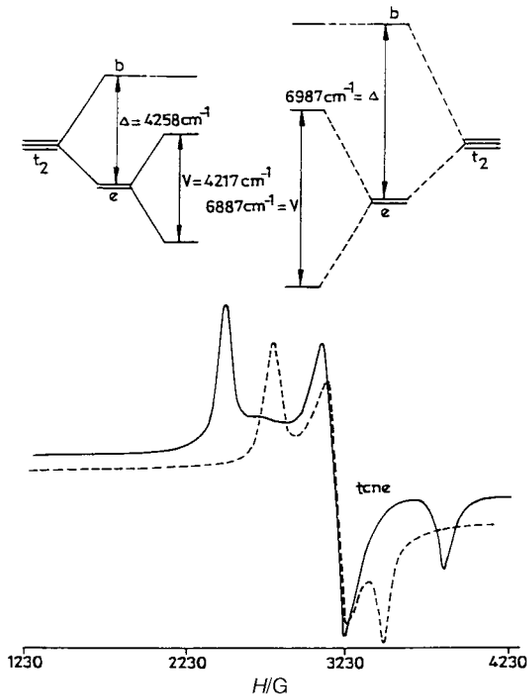

Fig. 6 X-Band EPR spectra and t_2 splittings of the complexes $[Ru^{III}(trpy)(L^3)Cl]ClO_4\cdot H_2O$ $\mathbf{3}^+$ (——) and $[Ru^{III}(trpy)(L^6)Cl]ClO_4\cdot H_2O$ $\mathbf{6}^+$ (------) in dichloromethane–toluene glass (77 K).

$k < 1.0$. The orbital reduction factor (k), axial distortion (Δ/λ), rhombic distortion (V/λ), and the two ligand field transitions (v_1/λ and v_2/λ) for complexes $\mathbf{3}^+$ and $\mathbf{6}^+$ are listed in Table 4. The value of the spin–orbit coupling constant (λ) of ruthenium(III) is taken as 1000 cm^{-1}.[33]

The v_2 band is detected in the expected region of the near-IR spectra of the complexes (Table 4). In view of the approximation involved in the theory, the agreement between the experimentally observed and the calculated v_2 value is excellent. Owing to instrumental wavelength scan limitation (maximum up to 2200 nm) it has not been possible to check the v_1 band. The distortion parameters (Δ and V) depicted in Table 4 reveal the presence of strong rhombic distortion in both complexes and in fact the rhombic distortion (V) is found to be similar to the axial distortion (Δ) (Table 4, Fig. 6). Therefore the complexes $[Ru(trpy)(L)(Cl)]^+$ $\mathbf{1}^+$–$\mathbf{6}^+$ can be considered as model ruthenium(III) complexes possessing a high degree of rhombic symmetry. The distortion values (Δ and V) are observed to be reasonably higher for $\mathbf{6}^+$ as compared to $\mathbf{3}^+$. The formation of the N=N group at the expense of the imine function of L^6 in complex $\mathbf{6}^+$ destroys the π conjugation of the chelate ring and this might have contributed to the observed higher degree of molecular distortion.

Spectroelectrochemical correlation

The lowest energy MLCT transition involves excitation of the filled t_2 electron of ruthenium(II) to the lowest π* orbital of the terpyridine ligand. The energy of the MLCT transition can be predicted with the help of observed electrochemical data by considering eqns. (1) and (2).[34] Here, $E^\circ_{298}(Ru^{III}–Ru^{II})$ and

$$v_{MLCT} = 8065(\Delta E^\circ) + 3000 \quad (1)$$

Table 5 Emission data[a]

Complex	λ_{max}/nm excitation	λ_{max}/nm emission	Quantum yield[b] (Φ)
3	575	665	0.28×10^{-1}
6	515	690	0.58×10^{-2}

[a] In ethanol–methanol (4:1 v/v) at 77 K. [b] Calculated by using eqn. (4) of text.

$$\Delta E^\circ = E^\circ_{298}(Ru^{III}–Ru^{II}) - E^\circ_{298}(L) \quad (2)$$

$E^\circ_{298}(L)$ are the formal potentials (in V) of the ruthenium(III)–ruthenium(II) couple and the first ligand reduction respectively and v_{MLCT} is the frequency of the lowest energy MLCT transition (in cm^{-1}). The factor 8065 in eqn. (1) is used to convert potential difference, ΔE, from volt to cm^{-1} and the term 3000 cm^{-1} is of empirical origin. The calculated and experimentally observed v_{MLCT} transition frequencies for the complexes are listed in Table 2. The calculated values lie within 900 cm^{-1} of the experimentally observed energies, which are in very good agreement with the previously observed correlation in other ruthenium complexes.[35]

Emission spectra

The complexes display very weak emissions at room temperature, therefore the emission properties of the complexes (**3** and **6**) have been studied in an optically dilute EtOH–MeOH (4:1 v/v) rigid glass at 77 K. Excitations of the complexes at the top of the lowest energy MLCT band exhibit moderately strong emissions near 700 nm (Table 5, Fig. 2). It is known that in polypyridine complexes, visible light absorption generally takes place into a ^{1}MLCT state whereas emission occurs from the ^{3}MLCT state. Therefore, the observed emissions are assigned to originate from the ^{3}MLCT excited sates.[36] The origin of the emission spectra is further confirmed by the excitation spectra of the corresponding solutions.

The quantum yields, Φ_{em}, were measured in EtOH–MeOH (4:1 v/v) rigid glass at 77 K relative to $[Ru(bpy)_3][PF_6]_2$ for which $\Phi_{em} = 0.35$.[37] Quantum yields are calculated using eqn. (3) as described previously,[14,38] where A is the absorbance

$$\Phi_{ems} = \Phi_{emr}(A_r/A_s)(I_s/I_r)(n_s/n_r)^2 \quad (3)$$

at the excitation wave length, I the integrated area of the emission band and n the refractive index of the solvent for the sample (subscript s) and the reference (subscript r), respectively. For the calculation of the quantum yield of the complexes, the excitation wavelengths are chosen such that standard reference and sample absorptions are equal. Since A_s and A_r are equal and the refractive indices are assumed to be similar, eqn. (3) can be modified to (4).

$$\Phi_{ems} = \Phi_{emr}(I_s/I_r) \quad (4)$$

The calculated quantum yields for the complexes are listed in Table 5. The complex incorporating the ligand of type **A** (**3**) is found to be the better emitter as compared to that having the ligand of type **B** (**6**). The presence of additional π conjugation in the chelate ring of L in complex **3** (C=CC=N) [which is

missing in **6** (C=CCN) due to internal transformation] might be one of the important contributing factors for the observed trend.

Chloride exchange reaction

The reaction of complexes $[Ru^{II}(trpy)(L)Cl]$, with aqueous $AgClO_4$ has been studied in order to prepare the aqua species $[Ru^{II}(trpy)(L)(H_2O)]^+$ *via* the chloride exchange route. However, instead of forming the expected stable ruthenium(II) aqua species the reaction leads to dimeric species of the type $[(trpy)(L)Ru^{III}(\mu\text{-}O)Ru^{III}(L)(trpy)]^{2+}$ with concomitant metal oxidation. The reaction here possibly proceeds through eqns. (5)

$$[(trpy)(L)Ru^{II}Cl] + Ag^+ \longrightarrow [(trpy)(L)Ru^{II}(H_2O)]^+ + AgCl \quad (5)$$

and (6). The source of oxidative equivalents in reaction (6) may

$$[(trpy)(L)Ru^{II}(H_2O)]^+ - 2e^- \longrightarrow [(trpy)(L)Ru^{III}(\mu\text{-}O)Ru^{III}(L)(trpy)]^{2+} \quad (6)$$

be either O_2 or ClO_4^-. Further investigations with the μ-oxo dimeric species are in progress.

Conclusion

We have observed the phenolato imine functions (L^-) incorporating CH_2 and NH spacers as a co-ligand in the ruthenium monoterpyridine [Ru(trpy)] core with respect to redox and spectroscopic aspects. The imine functions of type **B** are found to undergo internal imine ⟶ azo tautomerism. The presence of L (both **A** and **B**) facilitates the successive reversible ruthnium(III)–ruthenium(II) and ruthenium(IV)–ruthenium(III) processes and makes the complex environment susceptible to moderately strong emissions from the lowest energy MLCT transitions. The complexes possessing ligands of type **B** exhibit higher ligand field strength which has been reflected well in the metal redox processes as well as in the electronic transitions. In general a complex having a type **A** ligand (**3**) is more effective from the emission point of view compared to the other type of complex (**6**). The distortion parameters (Δ and V) of the trivalent complexes ($\mathbf{3}^+$ and $\mathbf{6}^+$) reveal the presence of a high degree of rhombicity in the complexes. Preliminary study indicates that in the presence of aqueous Ag^+ ion the complexes undergo aquation followed by dimerisation with concomitant metal oxidation.

Experimental

Materials

Commercial ruthenium trichloride (S.D. Fine Chemicals, Bombay, India) was converted into $RuCl_3 \cdot 3H_2O$ by repeated evaporation to dryness with concentrated hydrochloric acid. The complex $[Ru(trpy)Cl_3]$ was prepared according to the reported procedure.[7] 2,2′:6′,2″-Terpyridine, benzylamine and 2-hydroxy-5-nitrobenzaldehyde were obtained from Aldrich, USA. Other chemicals and solvents were reagent grade and used as received. Silica gel (60–120 mesh) used for chromatography was of BDH quality. For spectroscopic and electrochemical studies HPLC grade solvents were used. Commercial tetraethylammonium bromide was converted into pure tetraethylammonium perchlorate by an available procedure.[39]

Physical measurements

UV-visible spectra were recorded by using a Shimadzu-2100 spectrophotometer, FT-IR spectra on a Nicolet spectrophotometer with samples prepared as KBr pellets. Solution electrical conductivity was checked using a Systronic 305 conductivity bridge. Magnetic susceptibility was checked with a PAR vibrating sample magnetometer. NMR spectra were obtained with a 300 MHz Varian FT spectrometer. Cyclic voltammetric, differential pulse voltammetric and coulometric measurements were carried out using a PAR model 273A electrochemistry system. Platinum wire working and auxiliary electrodes and an aqueous saturated calomel reference electrode (SCE) were used in a three electrode configuration. The supporting electrolyte was $[NEt_4][ClO_4]$ and the solute concentration was 10^{-3} M. The half-wave potential E°_{298} was set equal to 0.5 ($E_{pa} + E_{pc}$), where E_{pa} and E_{pc} are the anodic and cathodic cyclic voltammetric peak potentials respectively. A platinum wire-gauze working electrode was used in coulometric experiments. All experiments were carried out under a dinitrogen atmosphere and uncorrected for junction potentials. The elemental analyses were carried out with a Carlo Erba (Italy) elemental analyser. The EPR measurements were made with a Varian model 109C E-line X-band spectrometer fitted with a quartz Dewar for measurements at 77 K (liquid nitrogen). The spectra were calibrated by using tetracyanoethylene (tcne) ($g = 2.0037$). The FAB mass spectra at 298 K were recorded on a JEOL SX 102/DA-6000 mass spectrometer.

Treatment of EPR data

An outline of the procedure can be found in our recent publications.[40] We note that a second solution also exists that is different from the chosen one, having small distortions and v_1 and v_2 values. The experimentally observed near-IR results clearly eliminate the solution as unacceptable.

Preparation of ligands and complexes

The ligands HL^{1-3} and HL^{4-6} were prepared by condensing benzylamine and phenylhydrazine respectively with the appropriate 2-hydroxyaldehydes and ketone at 273 K in methanol solvent. The recrystallised ligands were characterised by C, H, N analyses and NMR. The synthetic details are mentioned for one particular ligand (HL^2). Yields: 80–85%.

$C_{15}H_{15}NO$, HL^2. 2-Hydroxy acetophenone (2 g, 0.014 mol) was taken in 15 ml absolute ethanol and cooled at 273 K. Precooled benzylamine (1.5 g, 0.014 mol) was added dropwise to the above solution and the mixture stirred at 273 K for 1 h. The yellow precipitate thus formed was filtered off and washed thoroughly by ice-cold ethanol and dried in vacuum over P_4O_{10}. The product was finally recrystallised from hot ethanol. Yield: 2.64 g, 80%.

The complexes **1**–**6** were synthesized by following a general procedure. Details are given for one representative (**1**). Yields vary in the range 60–65%.

$[Ru^{II}(trpy)(L^1)Cl]$ 1. A 200 mg (0.454 mmol) quantity of $[Ru(trpy)Cl_3]$ was taken in 30 ml methanol and heated at reflux for 5 min. The ligand HL^1 (193 mg, 0.91 mmol) and $NaO\text{-}CH_3 \cdot 3H_2O$ (0.136 mg, 1.0 mmol) were added to the hot solution and the mixture was heated to reflux for 6 h. The initial light brown colour gradually turned to violet. The solvent was removed under reduced pressure. The dried product was purified by using a silica gel column. With benzene (as eluent) a light yellow solution due to excess of ligand was separated first and rejected. Using dichloromethane–acetonitrile (5:1) as eluent a violet band was separated, collected. Evaporation of the solvent under reduced pressure afforded a pure solid product which was recrystallised from dichloromethane–light petroleum (bp 60–80 °C) (1:6). Yield: 164 mg (62%).

The solid complexes **3** and **6** were directly separated from the reaction mixture. The precipitates thus formed were filtered off and washed thoroughly with methanol followed by distilled water. The solid complexes were dried *in vacuo* over P_4O_{10}. Finally the products were recrystallised from dichloromethane–light petroleum (1:6).

Table 6 Crystallographic data for $[Ru^{III}(trpy)(L^3)Cl]ClO_4 \cdot 0.5C_6H_6$ $\mathbf{3}^+$

Formula	$C_{32}H_{22}Cl_2N_5O_7Ru$
M	763.54
Crystal symmetry	Triclinic
Space group	$P\bar{1}$
a/Å	8.693(3)
b/Å	13.513(7)
c/Å	14.137(6)
α/°	99.88(4)
β/°	91.72(4)
γ/°	102.42(3)
T/K	293(2)
U/Å^3	1593.9(12)
Z	2
$R1$	0.046
$wR2$	0.112
Reflections collected/unique [R(int) = 0.0000]	5596/5596

Complexes $[Ru^{III}(trpy)(L^3)Cl]ClO_4 \cdot H_2O$ 3^+ and $[Ru^{III}(trpy)(L^6)Cl]ClO_4 \cdot H_2O$ 6^+. The oxidised complexes $[Ru^{III}(trpy)(L^3)Cl]ClO_4 \cdot H_2O$ $\mathbf{3}^+$ and $[Ru^{III}(trpy)(L^6)Cl]ClO_4 \cdot H_2O$ $\mathbf{6}^+$ were prepared *via* the chemical oxidations of bivalent congeners **3** and **6** using aqueous ammmonium cerium(IV) sulfate and ammonium cerium(IV) sulfate in 0.1 M $HClO_4$ respectively. Details are given for $\mathbf{3}^+$.

Complex **3** (100 mg, 0.16 mmol) was dissolved in 1:10 dichloromethane–acetonitrile (20 ml) and stirred magnetically at room temperature (298 K). To this was added dropwise 10 ml of aqueous $(NH_4)_4Ce(SO_4)_4 \cdot 2H_2O$ (203 mg, 0.32 mmol) solution. The violet solution gradually changed to green. The stirring was continued for 1 h. The solution was filtered through a fine frit, the volume reduced and a saturated aqueous solution of sodium perchlorate was added. The dark coloured solid mass thus obtained was filtered off, washed with ice-cold water, dried *in vacuo* over P_4O_{10} and subjected to chromatography on a silica gel column. A green band corresponding to $\mathbf{3}^+$ was eluted with 1:1 dichloromethane–acetonitrile. On evaporation the solid complex ($\mathbf{3}^+$) was obtained in 90% yield.

Crystallography

Single crystals of complex $\mathbf{3}^+$ were grown by slow diffusion of an acetonitrile solution of it in benzene followed by slow evaporation. Significant crystal data and data collection parameters are listed in Table 6. Absorption correction was done by ψ-scan measurement.[41] The data reduction was done by using MAXUS and structure solution and refinement used the programs SHELXS 97 and SHELXL 97 respectively.[42] The metal atom was located from the Patterson map and the other non-hydrogen atoms emerged from successive Fourier synthesis. The structure was refined by full-matrix least squares on F^2. All non-hydrogen atoms were refined anisotropically. Hydrogen atoms were included in calculated positions. The difference map revealed the presence of one-half molecule of lattice benzene solvent with one of the carbon atoms occupying a special position. This benzene molecule was refined isotropically with the aid of rigid group refinement using SHELXL 97.

CCDC reference number 186/1987.

See http://www.rsc.org/suppdata/dt/b0/b000257g/ for crystallographic files in .cif format.

Acknowledgements

Financial support received from the Department of Science and Technology, New Delhi, India, is gratefully acknowledged. The X-ray structural study was carried out at the National Single Crystal Diffractometer Facilities, Indian Institute of Technology, Bombay. Special acknowledgement is made to Regional Sophisticated Instrumental Center, RSIC, Indian Institute of Technology, Bombay for providing NMR and EPR facilities.

References

1 V. Balzani and F. Scandola, *Supramolecular Photochemistry*, Horwood, Chichester, 1991; K. Kalyanasundaram, *Coord. Chem. Rev.*, 1989, **28**, 2920; T. J. Meyer, *Pure Appl. Chem.*, 1986, **58**, 1193.
2 F. Scandola, C. A. Bignozzi and M. T. Indelli, *Photosensitization and Photocatalysis Using Inorganic and Organometallic Compounds*, eds. K. Kalyanasundaram and M.Gratzel, Kluwer, Dordrecht, 1993, p. 161.
3 Y. Xiong, X. F. He, X. H. Zhon, J. Z. Wu, X. M. Chen, L. N. Ji, R. H. Li, J. Y. Zhon and K. B.Yu, *J. Chem. Soc.*, *Dalton Trans.*, 1999, 19; V. W. W. Yam, B. W. K. Chu and K. K. Cheung, *Chem. Commun.*, 1998, 2261; B. J. Coe, D. A. Friessen, D. W. Thompson and T. J. Meyer, *Inorg. Chem.*, 1996, **35**, 4575; M. D. Ward, *Inorg. Chem.*, 1996, **35**, 1712; B. K. Santra, M. Menon, C. K. Pal and G. K. Lahiri, *J. Chem. Soc.*, *Dalton Trans.*, 1997, 1387; S. S. Kulkarni, B. K. Santra, P. Munshi and G. K. Lahiri, *Polyhedron*, 1998, **17**, 4365; D. Bhattacharyya, S. Chakraborty, P. Munshi and G. K. Lahiri, *Polyhedron*, 1999, **18**, 2951.
4 K. Hutchison, J. C. Morris, T. A. Nile, J. L. Walsh, D. W. Thompson, J. D. Petersen and J. R. Schoonover, *Inorg. Chem.*, 1999, **38**, 2516; J. Zadykowicz and P. G. Potvin, *Inorg. Chem.*, 1999, **38**, 2434; R. M. Berger and D. R. McMillin, *Inorg. Chem.*, 1998, **27**, 4245; R. R. Ruminski, S. Underwood, K. Vallely and S. J. Smith, *Inorg. Chem.*, 1998, **37**, 6528; E. C. Constable, C. J. Cathey, M. J. Hannon, D. A. Tocher, J. V. Walker and M. D. Ward, *Polyhedron*, 1998, **18**, 159; J. P. Sauvage, J. P. Collin, J. C. Chambron, S. Guillerez, C. Coudret, V. Balzani, F. Barigelletti, L. De Cola and L. Flamigni, *Chem. Rev.*, 1994, **94**, 993; A. Pramanik, N. Bag and A. Chakravorty, *J. Chem. Soc.*, *Dalton Trans.*, 1992, 97; C. A. Howard and M. D. Ward, *Angew. Chem.*, *Int. Ed. Engl.*, 1992, **31**, 1028; P. B. Sullivan, J. M. Calvert and T. J. Meyer, *Inorg.Chem.*, 1980, **19**, 1404.
5 A. Juris, V. Balzani, F. Barigelletti, S. Campagna, P. W. Belser and A. Zelewsky, *Coord. Chem. Rev.*, 1988, **84**, 85.
6 J. M. Calvert, J. V. Caspar, R. A. Binstead, T. D. Westmoreland and T. J. Meyer, *J. Am. Chem. Soc.*, 1982, **104**, 6620.
7 M. T. Indelli, C. A. Bignozzi, F. Scandola and J. P. Collin, *Inorg. Chem.*, 1998, **37**, 6084.
8 V. Grosshenny, A. Harriman and R. Ziessel, *Angew. Chem.*, *Int. Ed. Engl.*, 1995, **34**, 2705; F. Barigelletti, L. Flamigni, M. Guardigli, J. P. Sauvage, J. P. Collin and A. Sour, *Chem. Commun.*, 1996, 1329; L. Hammarstrom, F. Barigelletti, L. Flamigni, M. T. Indelli, N. Armaroli, G. Calogero, M. Guardilgli, A. Sour, J. P. Collin and J. P. Sauvage, *J. Phys. Chem. A*, 1997, **101**, 9061.
9 R. T. Morrison and R. N. Boyd, *Organic Chemistry*, Prentice Hall, Englewood Cliffs, NJ, 1992, 241.
10 A. Lobet, P. Doppelt and T. J. Meyer, *Inorg. Chem.*, 1988, **27**, 514.
11 N. Bag, S. B. Chowdhury, A. Pramanik, G. K. Lahiri and A. Chakravorty, *Inorg. Chem.*, 1990, **29**, 3014.
12 B. K. Santra, G. A. Thakur, P. Ghosh, A. Pramanik and G. K. Lahiri, *Inorg. Chem.*, 1996, **35**, 3050.
13 R. Samanta, P. Munshi, B. K. Santra, N. K. Lokanath, M. A. Sridhar, J. S. Prasad and G. K. Lahiri, *J. Organomet. Chem.*, 1999, **581**, 311.
14 K. D. Keerthi, B. K. Santra and G. K. Lahiri, *Polyhedron*, 1998, **17**, 1387.
15 S. Chakraborty, P. Munshi and G. K. Lahiri, *Polyhedron*, 1999, **18**, 1437.
16 D. A. Bardwell, A. M. W. Cargill Thompson, J. C. Jeffery, J. A. McCleverty and M. D. Ward, *J. Chem. Soc.*, *Dalton Trans.*, 1996, 873.
17 C. R. Hecker, A. K. I. Gushurst and R. D. McMillin, *Inorg. Chem.*, 1991, **30**, 538.
18 B. K. Santra and G. K. Lahiri, *J. Chem. Soc.*, *Dalton Trans.*, 1998, 139.
19 B. M. Holligan, J. C. Jeffery, M. K. Norgett, E. Schatz and M. D. Ward, *J. Chem. Soc.*, *Dalton Trans.*, 1992, 3345; R. Hariram, B. K. Santra and G. K. Lahiri, *J. Organomet. Chem.*, 1997, **540**, 155.
20 A. Bharath, B. K. Santra, P. Munshi and G. K. Lahiri, *J. Chem. Soc.*, *Dalton Trans.*, 1998, 2643.
21 R. P. Thummel and S. Chirayil, *Inorg. Chim. Acta*, 1988, **154**, 77.
22 B. K. Santra and G. K. Lahiri, *J. Chem. Soc.*, *Dalton Trans.*, 1997, 129.

23 N. Bag, G. K. Lahiri, S. Bhattacharya, L. R. Falvello and A. Chakravorty, *Inorg. Chem.*, 1988, **27**, 4396; G. K. Lahiri, S. Bhattacharya, S. Goswami and A. Chakravorty, *J. Chem. Soc.*, *Dalton Trans.*, 1990, 561.
24 T. B. Hedda and H. L. Bozec, *Inorg. Chim. Acta,* 1993, **204**, 103; G. B. Deacon, J. M. Patrick, B. W. Skelton, N. C. Thomas and A. H. White, *Aust. J. Chem.*, 1984, **37**, 929.
25 C. K. Johnson, ORTEP II, Report ORNL-5138, Oak Ridge National Laboratory, Oak Ridge, TN, 1976.
26 E. L. Lebeau, S. A. Adeyemi and T. J. Meyer, *Inorg. Chem.*, 1998, **37**, 6476.
27 G. K. Lahiri, S. Bhattacharya, M. Mukherjee, A. K. Mukherjee and A. Chakravorty, *Inorg. Chem.*, 1987, **26**, 3350.
28 R. Samanta, P. Munshi, B. K. Santra and G. K. Lahiri, *Polyhedron*, 1999, **18**, 995.
29 M. M. Taqui Khan, D. Chatterjee, R. R. Merchant, P. Paul, S. H. R. Abdi, D. Srinivas, M. R. H. Siddiqui, M. A. Moiz, M. M. Bhadbhade and K. Venkatasubramanian, *Inorg. Chem.*, 1992, **31**, 2711.
30 S. Chakraborty and G. K. Lahiri, unpublished work.
31 N. Bag, S. B. Chowdhury, A. Pramanik, G. K. Lahiri and A. Chakravorty, *Inorg. Chem.*, 1990, **29**, 5013.
32 P. Ghosh, A. Pramanik, N. Bag, G. K. Lahiri and A. Chakravorty, *J. Organomet. Chem.*, 1993, **454**, 273; N. J. Hill, *J. Chem. Soc.*, *Faraday Trans.*, 1972, **2**, 427; B. Bleaney and M. C. M. O'Brien, *Proc. Phys. Soc.*, *London*, *Ser. B*, 1956, **69**, 1216; J. S. Griffith, *The Theory of Transition Metal Ions*, Cambridge University Press, London, 1972, p. 364.
33 N. Bag, G. K. Lahiri, P. Basu and A. Chakravorty, *J. Chem. Soc.*, *Dalton Trans.*, 1992, 113.
34 S. Goswami, R. N. Mukherjee and A. Chakravorty, *Inorg. Chem.*, 1983, **22**, 2825; B. K. Ghosh and A. Chakravorty, *Coord. Chem. Rev.*, 1989, **95**, 239.
35 E. S. Dodsworth and A. B. P. Lever, *Chem. Phys. Lett.*, 1986, **124**, 152; M. A. Greaney, C. L. Coyle, H. A. Harmer, A. Jordan and E. I. Stiefel, *Inorg. Chem.*, 1989, **28**, 912.
36 L. M. Vogler and K. J. Brewer, *Inorg. Chem.*, 1996, **35**, 818.
37 G. A. Crosby and W. H. Elfring, Jr., *J. Phys. Chem.*, 1976, **80**, 2206.
38 R. Alsfasser and R.V. Eldik, *Inorg. Chem.*, 1996, **35**, 628.
39 D. T. Sawyer, A. Sobkowiak and J. L. Roberts, Jr., *Electrochemistry for Chemists*, 2nd ed., Wiley, New York, 1995.
40 A. Pramanik, N. Bag, G. K. Lahiri and A. Chakravorty, *J. Chem. Soc.*, *Dalton Trans.*, 1992, 101.
41 A. C. T. North, D. C. Phillips and F. S. Mathews, *Acta Crystallogr.*, *Sect. A*, 1968, **24**, 351.
42 G. M. Sheldrick, SHELXTL, Version 5.03, Siemens Analytical X-ray Instruments Inc., Madison, WI, 1994.